JOURNAL OF VIROLOGY, Nov. 1999, p. 9568–9575 Vol. 73, No. 11
0022-538X/99/$04.00+0

Observation of Measles Virus Cell-to-Cell Spread in Astrocytoma Cells by Using a Green Fluorescent Protein-Expressing Recombinant Virus

W. PAUL DUPREX,[1]* STEPHEN MCQUAID,[2] LARS HANGARTNER,[3] MARTIN A. BILLETER,[3] AND BERT K. RIMA[1]

School of Biology and Biochemistry, The Queen's University of Belfast, Belfast BT9 7BL,[1] and Neuropathology Laboratory, Royal Group of Hospitals Trust, Belfast BT12 6B1,[2] Northern Ireland, United Kingdom, and Institut für Molekularbiologie, Universitat Zürich-Irchel, 8057 Zürich, Switzerland[3]

Received 21 April 1999/Accepted 22 July 1999

A recombinant measles virus (MV) which expresses enhanced green fluorescent protein (EGFP) has been rescued. This virus, MVeGFP, expresses the reporter gene from an additional transcription unit which is located prior to the gene encoding the measles virus nucleocapsid protein. The recombinant virus was used to infect human astrocytoma cells (GCCM). Immunocytochemistry (ICC) together with EGFP autofluorescence showed that EGFP is both an early and very sensitive indicator of cell infection. Cells that were EGFP-positive and ICC-negative were frequently observed. Confocal microscopy was used to indirectly visualize MV infection of GCCM cells and to subsequently follow cell-to-cell spread in real time. These astrocytoma cells have extended processes, which in many cases are intimately associated. The processes appear to have an important role in cell-to-cell spread, and MVeGFP was observed to utilize them in the infection of surrounding cells. Heterogeneity was seen in cell-to-cell spread in what was expected to be a homogeneous monolayer. In tissue culture, physical constraints govern the integrity of the syncytia which are formed upon extensive cell fusion. When around 50 cells were fused, the syncytia rapidly disintegrated and many of the infected cells detached. Residual adherent EGFP-positive cells were seen to either continue to be involved in the infection of surrounding cells or to remain EGFP positive but no longer participate in the transmission of MV infection to neighboring cells.

Measles virus (MV) is a morbillivirus which belongs to the family *Paramyxoviridae* and is therefore a member of the *Mononegavirales*, all of which have largely similar replication strategies (39). Its single-stranded RNA genome is composed of 15,894 nucleotides and contains a total of six transcription units, which are separated by intergenic trinucleotide spacers. The transcription units encode the six major structural proteins of the virus. Due to RNA editing and the use of multiple translation start sites, at least two further proteins, designated V and C, are generated from the genome (4, 21). Transcription occurs by sequential, interrupted copying from the six genes. A gradient of transcripts, which decrease in abundance depending on the distance of the gene from the single 3′ terminal promoter, is generated (10). Alterations in the MV transcription gradient have been observed in infected human astrocytoma cells (44), and astrocytes have been shown to be infected by MV in vivo (1, 29, 33). How these cells become infected is unclear. Neurones are also infected in vivo, and transynaptic spread of the virus in the central nervous system (CNS) has been suggested but remains unproved (1).

Full-length infectious clones are available for a number of negative-stranded RNA viruses, including MV (11, 22, 40, 48, 57). Reverse genetics has demonstrated that the genomes of members of the *Mononegavirales*, for example, vesicular stomatitis virus, can tolerate substantial rearrangements in gene order (56). Additional transcription units (ATUs) have been added to respiratory syncytial virus and vesicular stomatitis virus, and the foreign genetic material is stably retained after many cycles of multiplication in cultured cells (7, 47). Recently, interleukin-12 has been incorporated into the MV genome. The additional sequences represent an additional 20% of the genome, and they were retained for at least 10 passages (50). These observations indicate that negative-stranded genomes exhibit a remarkable degree of flexibility in both their length and organization. In addition, the MV rescue system (40) has been used to investigate the function of the M, F, H, P, V, and C virus proteins (8, 9, 41, 43); pathogenesis (8, 17, 52, 54); and virus maturation and assembly (49).

Green fluorescent protein (GFP) has recently become a widely used reporter gene. The protein's autofluorescence has been enhanced by mutating amino acids surrounding the chromophore to alter the excitation peak (23), and its expression levels have been increased by changing the codons of the gene to those which are frequently represented in human genes (58). These modifications resulted in the production of an enhanced GFP (EGFP) variant. Both GFP and EGFP genes have been inserted into a number of viral genomes, for example, those of herpes virus 1 and mouse hepatitis virus (19, 20). Simian varicella-zoster virus pathogenesis and latency have been studied in experimentally infected animals following GFP insertion by homologous recombination (31). Additionally, GFP has been fused to the Tat protein of human immunodeficiency virus type 1 to study trafficking and intracellular localization (51).

It is generally assumed that MV is propagated in the CNS in the absence of budding, possibly by cell-to-cell fusion, and the intimate relationship which is known to exist between astrocytes and neurones (16, 25) may facilitate cell-to-cell spread. In

* Corresponding author. Mailing address: School of Biology and Biochemistry, The Queen's University of Belfast, Medical Biology Centre, 97 Lisburn Rd., Belfast BT9 7BL, Northern Ireland, United Kingdom. Phone: 01232 272060. Fax: 01232 236505. E-mail: p.duprex@qub.ac.uk.

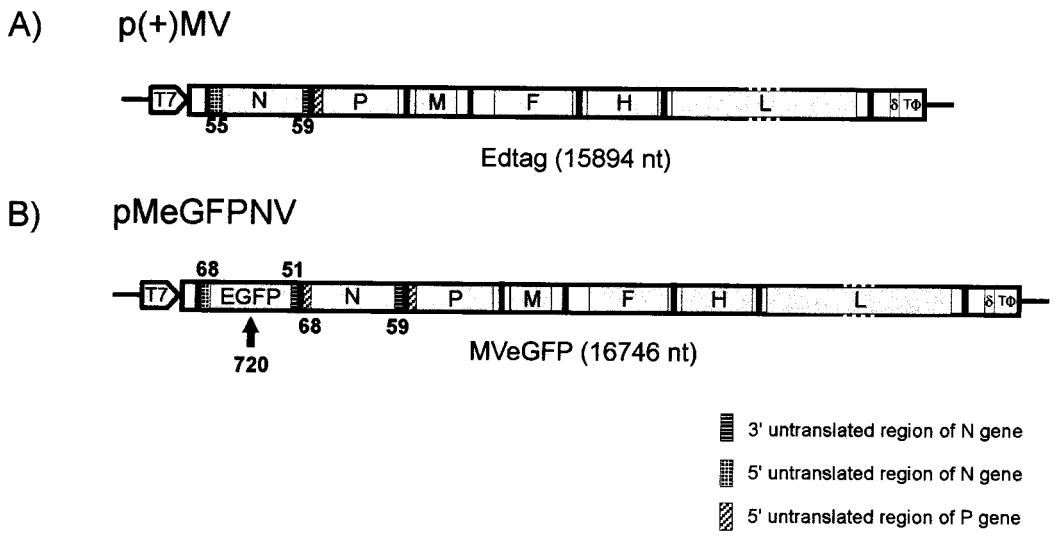

FIG. 1. Schematic representation of the full-length MV plasmids used for virus rescue. The solid lines indicate the positions of the intergenic trinucleotide spacers. The positions of the T7 promoter, hepatitis delta ribozyme (δ), and T7 terminator (TΦ) are indicated (not to scale). Open reading frames encoding the virus structural genes are shaded, and their flanking untranslated regions are represented as open boxes. The genome length of each virus is given in nucleotides (nt). (A) Structure of p(+)MV encoding the MV Edmonston B strain antisense genome (Edtag). The sizes of the 3′ and 5′ untranslated regions of the N gene are indicated. (B) Structure of pMeGFPNV encoding the MV Edmonston B strain antisense genome with an ATU which is composed of the open reading frame of EGFP flanked by sequences based on the 3′ and 5′ untranslated regions of the N gene. A total of 852 additional base pairs are present in pMeGFPNV. The sizes of the untranslated regions are indicated below and above the EGFP and N gene segments respectively.

this paper we report on the utilization of a recombinant MV which expresses EGFP to examine astrocytoma cell infection. We show that EGFP is a very early indicator of cell fusion and infection compared to the immunocytochemical (ICC) detection of nucleocapsid protein, the most abundant MV protein. Finally, we show that the cellular processes of these glial cells mediate MV spread in tissue culture.

MATERIALS AND METHODS

Cells and viruses. The MV rescue cell line, 293-3-46, was maintained as previously described (40). Vero cells were grown in Dulbecco's modified Eagle medium (DMEM; Gibco) containing 8% newborn-calf serum (NCS; Gibco). These were used for the growth of recombinant MVs, which were propagated in DMEM containing 2% NCS. Stocks of rescued, plaque-purified viruses were produced by passage in Vero cells. Titers were obtained by 50% endpoint dilution assays and are expressed in 50% tissue culture infectious doses determined by the method of Reed and Muench (42). Human astrocytoma cells (GCCM) were obtained from an anaplastic astrocytoma grade IV and were grown in DMEM supplemented with 5% fetal calf serum (Gibco).

Plasmids and virus rescue. Plasmid pMeGFPNV includes the antigenome of MV with an insertion containing the open reading frame of EGFP flanked by the 3′ and 5′ untranslated regions of the N gene. The cloning strategies used in the generation of pMeGFPNV will be reported elsewhere (23a). The ATU is composed of 852 nucleotides, and pMeGFPNV conforms to the rule of six (28). The insertion was made into the full-length infectious clone of MV, p(+)MV (EMBL accession no. Z66517), between the 3′ end and the gene encoding the nucleocapsid protein. Recombinant virus was recovered from this plasmid by using the 293-3-46 rescue cell line, which stably expresses T7 RNA polymerase and the N and P proteins of MV (40). Briefly, the cell line was transfected with pMeGFPNV (5 μg) and pEMCLa (10 ng), which expresses the MV polymerase protein under the control of the T7 promoter, using a calcium phosphate transfection procedure. The cell sheets were monitored microscopically each day for the appearance of syncytia. Autofluorescence within these syncytia, indicating EGFP expression, was verified with an inverted UV microscope (Leica). Virus stocks were produced following plaque purification, and titers of approximately 5×10^5 50% tissue culture infectious doses/ml were obtained. The stocks were stored at −70°C. Fluorescence microscopy was used routinely to determine that EGFP expression was retained upon virus passage and to ensure that mutants which had lost the ability to express EGFP were present below the limit of detection.

Immunofluorescence and confocal microscopy. GCCM cells were grown on glass coverslips to 80% confluency. The monolayers were rinsed with maintenance medium, and the cells were infected with MVeGFP at a multiplicity of infection (MOI) of 0.01 and incubated for 1 h at 37°C. After this time, unadsorbed virus was removed, maintenance medium containing 2% NCS was added, and the cells were incubated for 50 to 60 h at 37°C. The presence of EGFP-positive cells was verified by UV microscopy, and the cells were then fixed for 10 min in 4% paraformaldehyde. Infected cells were observed at a time point similar to that following the parental Edtag virus infection, and it appears that the presence of EGFP in an ATU does not significantly impede virus replication (23a). Anti-MV nucleocapsid (N) monoclonal antibody (Seralabs) was diluted 1:1,000 in phosphate-buffered saline (PBS). Anti-tubulin monoclonal antibody (Sigma) was diluted 1:1,500 in PBS. Human hyperimmune serum was obtained from a patient with confirmed subacute sclerosing panencephalitis (SSPE) and was used at a dilution of 1:1,000 in PBS. Primary antibodies were added to the cells on the glass coverslips and incubated for 1 h at 37°C. Incubation was followed by three 5-min washes with PBS. Secondary antibodies, CY3-conjugated sheep anti-mouse (Sigma; 1:40) and CY5-conjugated goat anti-human (Amersham; 1:40), were diluted in PBS and added to the coverslips, which were then incubated for 1 h at 37°C. The coverslips were washed three times in PBS and mounted with Citifluor (Amersham). A Leica TCS/NT confocal microscope equipped with a krypton-argon laser as the source for the ion beam was used to examine the samples for fluorescence. CY5-stained samples were imaged by excitation at 647 nm with a 664- to 696-nm-long-pass emission filter, and CY3-stained samples were imaged by excitation at 568 nm with a 564- to 596-nm-band-pass emission filter. EGFP was visualized by virtue of its autofluorescence by excitation at 488 nm with a 506-538 band-pass emission filter.

Vital fluorescent microscopy. Astrocytoma cells (GCCM) were cultured to 60% confluence in 25-cm^3 tissue culture flasks. The cells were infected at an MOI of 0.01 with MVeGFP. An inverted UV microscope was used to monitor the monolayers for the appearance of single infected cells. The flasks were oriented on the microscope stage, which was marked to permit the repeated observation of the chosen groups of infected cells in the monolayers. Autofluorescent images of the cells were collected by confocal scanning laser microscopy (CSLM). All settings on the microscope were kept constant, and the laser intensity was adjusted, if necessary, to maintain similar output levels. The flasks were handled with extreme care to avoid disruption of the infected cell structures. Immediately after the image was recorded, the infected monolayers were returned to 37°C for further incubation. The stored images were used throughout the experiment to precisely reorient the cells. Observations were made over a period of 50 h at intervals of between 2 and 4 h.

RESULTS

Recombinant MVeGFP infects astrocytoma cells. Recombinant MV expressing EGFP was recovered 6 days posttransfection. Figure 1 shows a schematic representation of the plasmid pMeGFPNV, from which this virus was derived. In addition to the complete MV genome pMeGFPNV contains an ATU

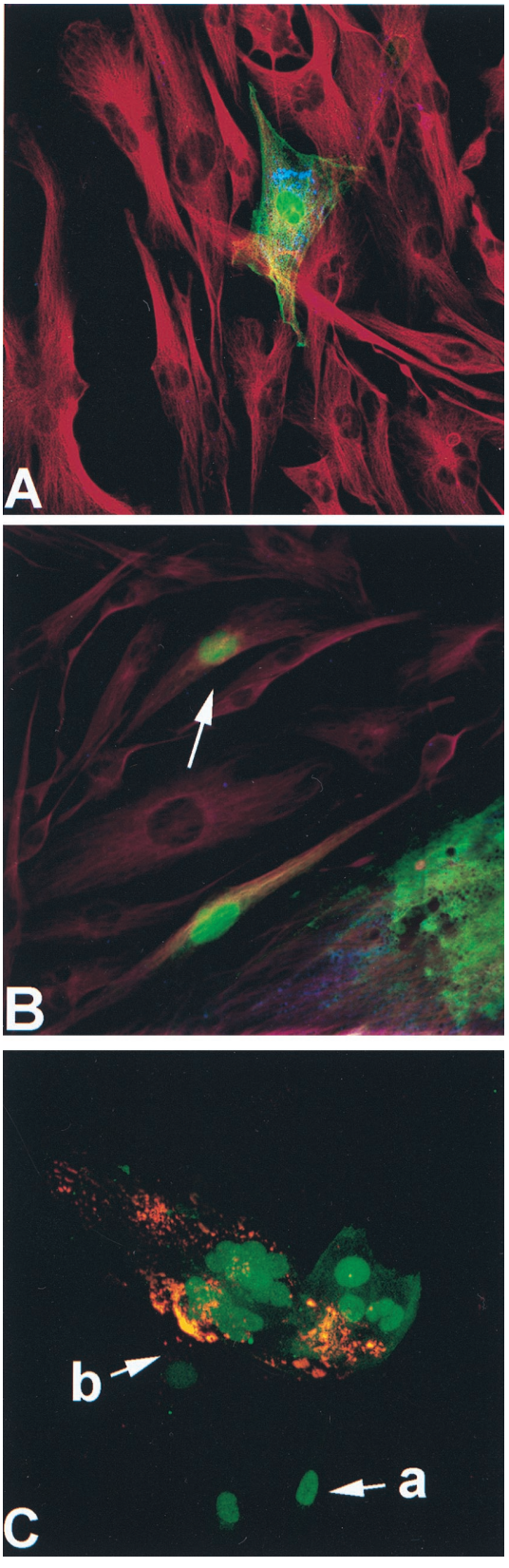

FIG. 2. Immunoreactivity and autofluorescence in astrocytoma cells infected with MVeGFP. GCCM cells were infected with MVeGFP at an MOI of 0.01 for 50 h. The cells were fixed and examined by CSLM for autofluorescence and immunoreactivity. The micrographs represent an 8- to 10-μm composite optical section. The images were obtained in double- or triple-excitation mode. MV antigens were detected with either human SSPE antiserum or a monoclonal antibody which recognizes the MV nucleocapsid protein. EGFP was detected by virtue of its autofluorescence, and the cell cytoskeleton was visualized with a monoclonal antibody specific for tubulin. (A) A single cell infected with MVeGFP. MV antigens, detected with SSPE antiserum (blue), tubulin (red), and EGFP (green), are shown. (B) A single cell infected with MVeGFP (arrow) in close proximity to a large syncytium; MV antigens, detected with SSPE antiserum (blue), tubulin (red), and EGFP (green), are shown. MV antigen was not observed in the single infected cell. (C) Cells in the early stages of MVeGFP infection. MV nucleocapsid antigen (red) and EGFP (green) are shown. Arrow a indicates two EGFP-positive and MV antigen-negative cells. Arrow b indicates an EGFP-positive cell which also stains positive for a small number of MV cytoplasmic inclusion bodies. The three cells indicated by arrows are connected to the syncytium, in which relatively large amounts of viral antigen are detected. Magnification, ×40.

composed of the complete EGFP open reading frame flanked by 3′ and 5′ untranslated regions which are based largely on those of the nucleocapsid gene. The ATU is located in the 3′ terminal region of the genome, prior to the N gene. Infectious virus was recovered at a time point similar to that for Edtag virus (control), indicating that the high-level expression of the reporter gene and surrounding untranslated sequences has no major effects on virus replication.

In this study the recombinant virus, MVeGFP, was used to infect GCCM cells in order to assess the distribution of EGFP and viral antigens with respect to the cytoskeleton. The latter was visualized with an anti-tubulin monoclonal antibody. Figure 2A shows a single infected astrocytoma cell surrounded by uninfected cells. Diffuse EGFP autofluorescence was detected throughout the cytoplasm and seemed to accumulate in the nucleus. The figure is a composite of several images representing different depths within the tissue. Examination of the individual sections indicated that EGFP was present throughout the nucleus. Intranuclear localization of the reporter protein to any particular area of the nucleus, or to the nuclear membrane, was not observed. MV antigens were detected with an SSPE antiserum and visualized with an anti-human CY5-conjugated secondary antibody. A punctuate staining pattern was observed, which is characteristic of cytoplasmic inclusion bodies which contain N protein encapsidating viral RNA (1). The inclusion bodies were seen to localize in the perinuclear region of the infected cell. Tubulin was visualized indirectly with a CY3-conjugated secondary antibody. This gave an indication of the overall GCCM cell morphology, and extended astrocytic processes, which are typical of an astrocytoma cell line, were seen to connect the cells. Observing tubulin in conjunction with EGFP indicated that every part of the cytoplasm contained the reporter protein. No effects on the cytoskeleton were observed within the infected cells.

EGFP is an early indicator of MV cell infection. From initial observations of infected cells it appeared that EGFP was present in cells which were negative for MV antigen. One of two mechanisms could cause a cell to be EGFP positive and MV antigen negative. First, due to the location of the EGFP gene at the 3′ end of the genome and the consequent high levels of expression, detection of autofluorescence could be predicted to be sensitive in comparison to MV antigen detection by ICC methods. In this instance detection of EGFP would sensitively reflect the rate of replication within the infected cell. In a second scenario EGFP may passively enter from earlier infected cells into new cells soon after MV-induced cell fusion due to the contiguity of the cytoplasm. In this case, the presence of EGFP would not reflect the amount of viral replication within the newly infected cell. In order to distinguish between these two possibilities, we made a direct comparison between EGFP autofluorescence and the standard

ICC detection of MV in infected cells. The most abundant virus proteins, N and P, were visualized by indirect immunofluorescence in GCCM cells infected with MVeGFP, as described above. A triple-labelled composite image is shown in Fig. 2B. Viral antigen and EGFP autofluorescence were observed within the syncytium. A single infected cell, which is negative for viral antigen, is indicated. Due to the cytoskeletal staining, it is clear that this cell is isolated from the nearby syncytium and is in the initial stages of infection. This type of cell was frequently observed by confocal microscopy. The possibility that EGFP can passively enter recently fused cells is also indicated in this figure. A cell was observed, at the periphery of the syncytium, which appeared to be antigen negative. To clarify this situation we used ICC to stain cells infected with MVeGFP. Nucleocapsid protein was detected with a highly sensitive anti-N monoclonal antibody recognized by a CY3-conjugated sheep anti-mouse secondary antibody. CY3 is a very stable fluorescent conjugate with the additional advantage that, unlike CY5, it can be visualized directly by UV microscopy. Figure 2C also shows that EGFP is detected in MVeGFP-infected cells which are negative for MV N protein. Two cells are shown in the very early stages of infection. Fusion appears to have only recently taken place, as the cells are physically joined to the syncytium. Antigen-containing intracytoplasmic inclusions are usually found surrounding the nuclei, and these were clearly observed in the main body of the syncytium. A low level of positive staining for nucleocapsid was also observed in cells on the periphery of the syncytium (Fig. 2C). The protein is present in smaller amounts, and we believe that these cells, like the N protein-negative/EGFP-positive cells, are in early stages of infection. Three phases of MV infection are therefore shown in Fig. 2C. First are the cells within the syncytium which are producing large amounts of MV proteins. Second are the cells which are EGFP positive but have much lower levels of N antigen than those within the main body of the syncytium. In this case EGFP autofluorescence clearly shows that these cells are infected even though viral antigen levels are low. Third are the cells which lack the most abundant viral protein, N, but, because of the presence of EGFP, must be fused to the syncytium. This was confirmed by phase microscopy. Detection of these cells at this early stage of infection has not been possible previously.

Processes mediate the rapid spread of MVeGFP from cell to cell. From the above-mentioned results it appears that EGFP autofluorescence within fixed tissue is a more sensitive indicator of infection than ICC. Fixed tissues, however, do not allow cell-to-cell spread of the virus to be examined. The availability of the recombinant virus, MVeGFP, gives the first opportunity of making observations of the spread of MV from one individual cell to another in real time.

GCCM cells were infected at a low MOI, and single infected cells were observed by UV microscopy from 60 h postinfection. Three representative time courses of MVeGFP-infected centers illustrating the variation in progression of the virus from cell to cell are shown in Fig. 3. Observations were made at appropriate time points over a total period of 50 h. In Fig. 3A, two infectious centers are shown. The upper left center is simply a single infected cell, whereas in the lower-right infectious center fusion with a neighboring cell has already occurred. MV-infected cells have fused with uninfected cells via the connecting processes, leading to the formation of a syncytium which is composed of two cells. Where these processes are in intimate contact with other cells, the fusion is rapid, and it can be seen that after 8.5 h many more cells are infected (74.5 h post infection [p.i.]). In many cases extended cellular processes of uninfected cells passed above or below the infected GCCM cells, and these seemed to be refractile to infection. This may indicate that intimate cell contact with the end of the processes is a prerequisite for fusion. As time proceeds and more cells are recruited into the syncytium, physical constraints lead to its breakdown. By 95 h p.i., the lower-right syncytium has lysed and only a few residual infected cells remain. By this time point the two infectious centers have merged.

A different pattern of spread was observed when the initial infection occurred in a cell which was in more intimate contact with the cell bodies of the surrounding cells (Fig. 3B). In this instance, by 66 h p.i. fusion of the surrounding cells produced a syncytium in which the brightly fluorescent nuclei clustered in the center. Diffuse EGFP autofluorescence was visible in the cytoplasm of the syncytium. More cells were infected at this time point, particularly at the periphery of the syncytium, than in the time course presented in Fig. 3A. By 71 h p.i., cytoplasmic bridges had formed. These were derived from the contracted cytoplasm of fused cells and do not represent astrocyte processes. As time proceeds (76.5 h p.i.), more cells become infected via interconnecting processes and the cytoplasmic bridges are seen to become narrower. By 79 h p.i., the cytoplasmic bridges ruptured, causing the fused structure to disintegrate, and a hole was left in the monolayer. The majority of the surrounding infected cells remained adherent, and these residual cells were observed for a further 37 h. The infection proceeded in a fashion similar to that shown in Fig. 3A by further outward spread via processes. Observations of other infected centers indicated that in some cases these residual cells, which remained after a syncytium had burst, could no longer fuse with surrounding cells, and the infection process appeared to terminate (data not shown).

Finally, a very different situation was observed for one of the infectious centers which had been selected for observation at 66 h p.i. (Fig. 3C). In this case, repeated observations over 24 h showed no progression of the infection, despite the presence of surrounding GCCM cells which were readily observed by phase microscopy. During this period, slight differences were observed in the overall shape of the infected cells, indicating that they had moved slightly with respect to each other (66, 77, and 90 h p.i.). At 90 h p.i., the cells were no longer observed every 2 to 4 h. Interestingly, in the final observation, at 116 h p.i., many of the surrounding cells were seen to be infected. This indicates that at some stage the impediment to infection of these cells was surmounted and a burst of infection followed as detailed in the series in Fig. 3A.

Partially autofluorescent cells were never observed in repeat observations. It appears that upon fusion an influx of EGFP from the infected cells causes the rapid dissemination of EGFP into the cell cytoplasm. Autofluorescence is subsequently detected, first in the nucleus, possibly due to nonspecific accumulation, and secondly throughout the cytoplasm, rather than at the site of cell fusion. This agrees with the observations which were made in fixed cells (Fig. 2). All the main stages in the spread of MVeGFP infection are shown in Fig. 4, and the role of cellular processes is particularly evident. At 66 h p.i. two infected cells were visible, and these were connected by an astrocytic process. Four hours later (70 h p.i.), a further two cells were infected, and the extended process from one of these cells is indicated. By 74 h p.i., the neighboring cell was in the very early stages of infection, as indicated by EGFP autofluorescence in the nucleus. Cytoplasmic staining was not observed. Five hours later, EGFP autofluorescence in this cell was much more intense and a process from the cell was now visible. Two hours later (81 h p.i.), the processes were more defined, although at this stage in the time course no new cells

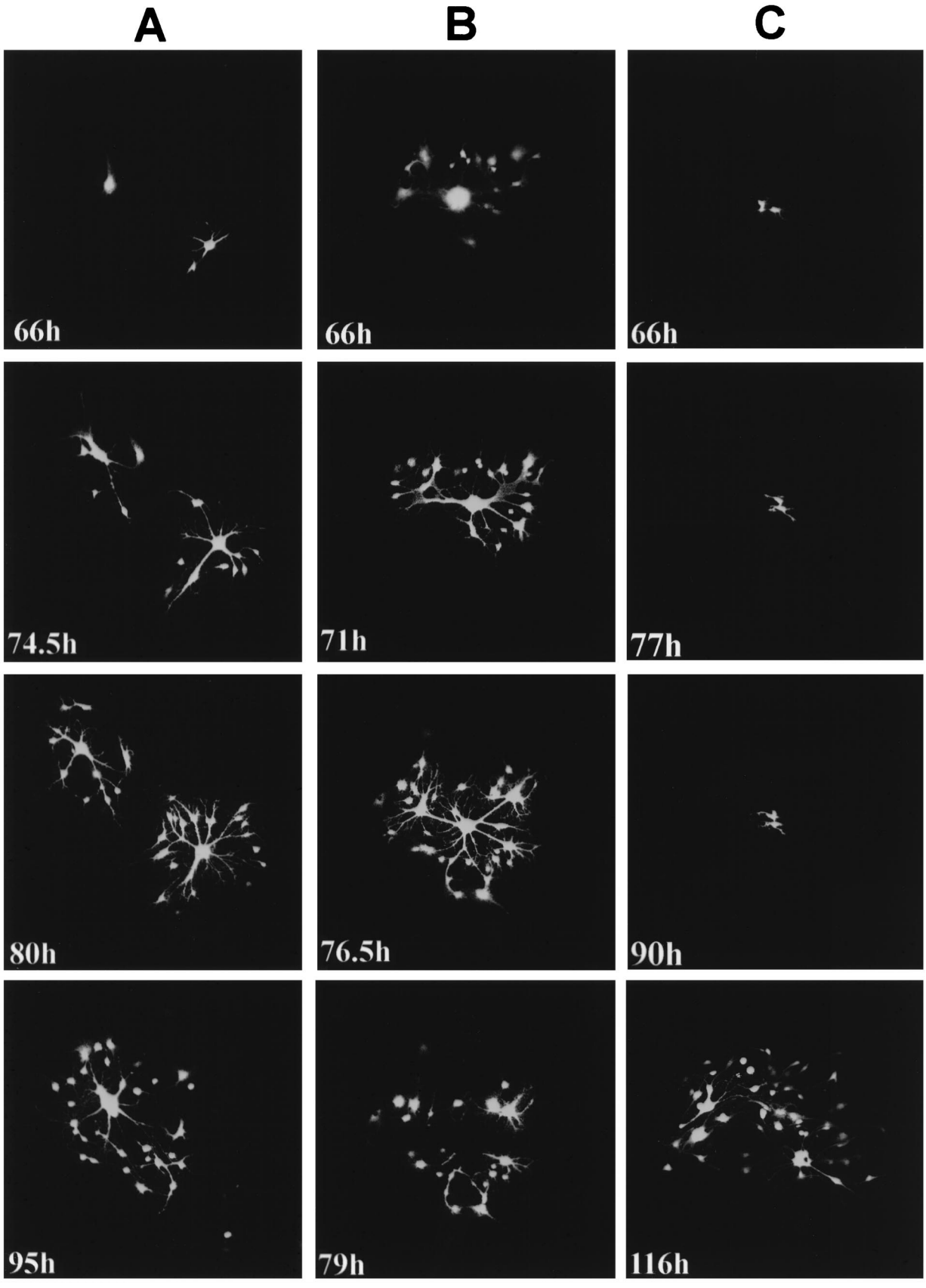

FIG. 3. Variation in the cell-to-cell spread of MVeGFP in astrocytoma cells (see text for details). GCCM cells at 60% confluency were infected with MVeGFP at an MOI of 0.01. Infected cells were identified by UV microscopy, and the positions of the infectious centers in the monolayer were marked to aid in their reidentification throughout the time course. Three representative time course experiments are shown (A, B, and C), and each demonstrates the variation in the virus spread from cell to cell. The images were collected in a single optical section by CSLM in single-excitation mode. The number of hours postinfection at which each autofluorescent image was collected is indicated. EGFP autofluorescence is shown in false-white color. Magnification, ×10.

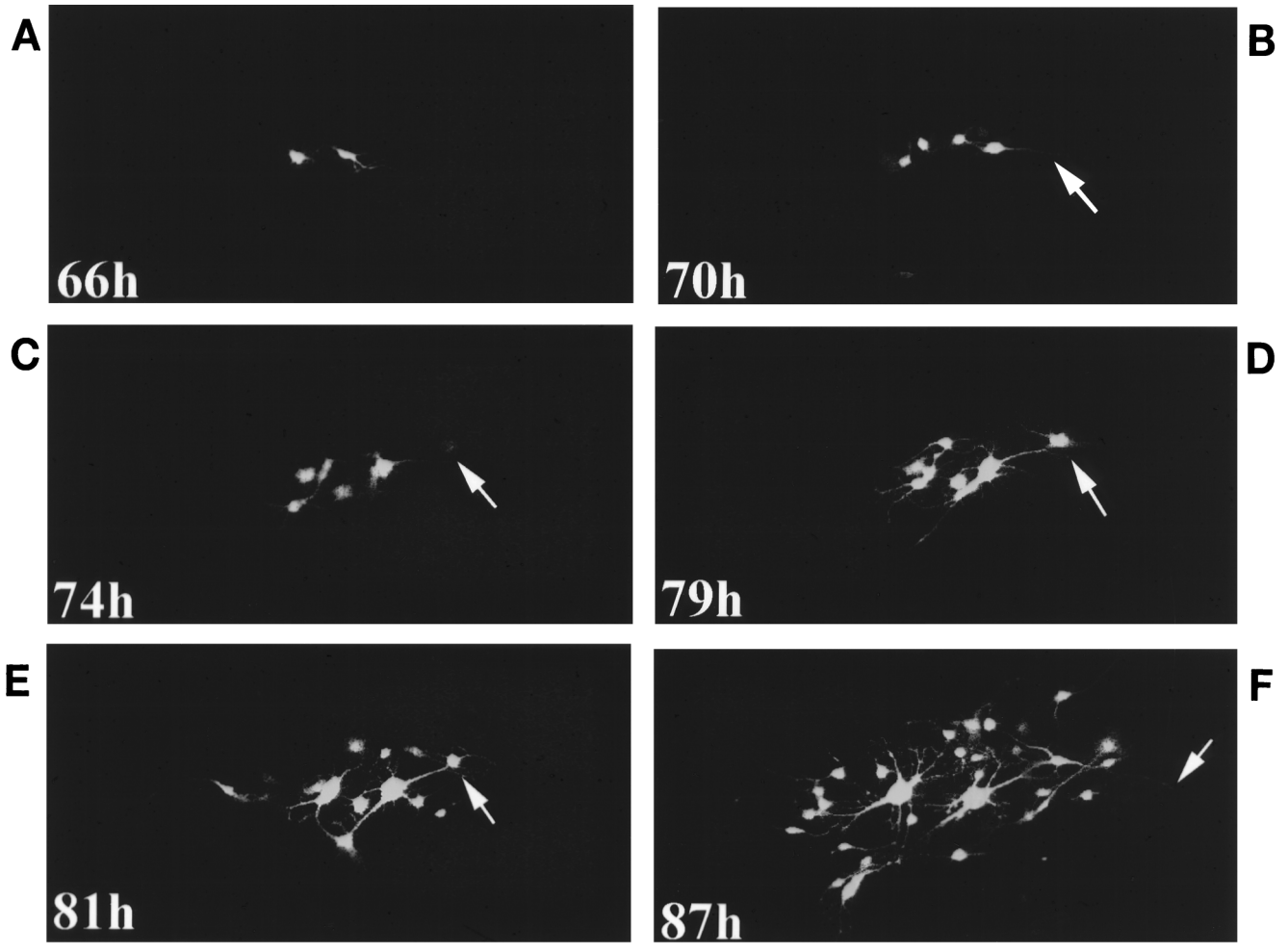

FIG. 4. Process-mediated cell-to-cell spread in GCCM cells infected with MVeGFP. Astrocytoma cells at 60% confluency were infected with MVeGFP at an MOI of 0.01. (A) Two infected cells were identified by UV microscopy at 66 h p.i. and observed for a further 21 h at approximately 4-h intervals. (B) The arrow indicates an extended astrocyte process of a newly infected cell. (C) The arrow indicates the weakly autofluorescent nucleus of a cell in the very early stages of infection. (D and E) The arrows indicate the same nucleus 5 and 7 h later. (F) The arrow indicates an extended astrocytic process emanating from the cell indicated in panels D and E. EGFP-autofluorescent images were collected as single optical sections by CSLM and are shown in false-white color. Magnification, ×15.

had been infected. Finally, by 87 h p.i. a number of connected cells were infected and an extended process was visualized by EGFP autofluorescence. This series clearly shows that processes play an important role in cell-to-cell spread, especially as it should be noted that uninfected cells were present between the autofluorescent cells.

DISCUSSION

Astrocyte infection by morbilliviruses has been demonstrated both in vivo and in vitro (1, 5, 12, 26, 30, 33, 38, 45, 55). The predominant cell types infected in SSPE are neurones and oligodendrocytes (24). Infected glial cells have been detected by immunohistochemistry, albeit at lower frequencies (1, 30, 33), but the degree of astrocyte infection in vivo remains controversial (6, 18, 29, 32). Canine distemper virus, another morbillivirus, also infects astrocytes. The virus persists in the CNS, replicating and spreading in astrocytes without eliciting an inflammatory response (5, 26, 55). MV infects rat astrocytes in tissue culture (45). A distinct alteration in the transcription gradient of MV monocistronic messages is observed in experimentally infected rodents (46), and this mirrors the in vivo situation in brain tissue from patients with SSPE and measles inclusion body encephalitis (10). Alterations in the transcription gradient also occur in cultured human astrocytoma cells (44). In light of these observations, we were first interested to examine if MVeGFP could infect the human astrocytoma cell line GCCM and, if so, at what stage in the infection EGFP autofluorescence could be detected. Secondly, we wished to examine, in real time, the cell-to-cell spread of MV in this glial cell line.

GCCM cells were found to be readily infectable by MVeGFP, and a diffuse cytoplasmic autofluorescence was observed (Fig. 2). We have also verified that nontransformed fetal astrocytes could be productively infected with MVeGFP. The infection was highly fusogenic (data not shown). It was evident that EGFP autofluorescence served as a very early indicator of GCCM cell infection. Indeed, EGFP autofluorescence occurred in cells in which MV antigen was not detectable by ICC staining with a highly specific monoclonal antibody against the most common viral antigen, the nucleocapsid protein. This can be explained in two ways: (i) the influx of EGFP from infected cells upon fusion or (ii) the ability to sensitively detect the reporter gene by confocal microscopy soon after

primary infection before viral antigens reach detectable levels. Both were demonstrated. Therefore, expression of EGFP by MVeGFP serves to locate cells which are in the early stages of infection, and this virus will be an invaluable tool to investigate MV spread in vitro and possibly in vivo.

EGFP was seen to accumulate in the nuclei of GCCM cells at a very early stage of cell infection. When nonenhanced GFP was expressed in BHK21 cells with the Semliki Forest virus system it was present diffusely throughout the cytoplasm and was also seen to enter the nucleus (2). Our results seem to indicate that a nonspecific mechanism may lead GCCM cells to accumulate GFP in the nucleus. Recombinant EGFP-expressing pseudorabies virus has also been generated (27). In this system it does not appear that EGFP accumulates in the nucleus, although different cell lines were used. A monoclonal antibody was used to detect EGFP by indirect immunofluorescence in MDBK cells infected with this recombinant virus. Interestingly, when EGFP autofluorescence was compared with ICC, the fluorescein isothiocyanate-labelled fluorescence was much brighter despite the use of a strong gG promoter. This limits the use of the EGFP reporter in this system.

In SSPE it is assumed, although not yet proven, that MV spreads transneuronally from cell to cell, as no budding is seen from the surfaces of infected cells (14, 37). Virus isolated from various parts of infected brains of patients with SSPE is clonal, suggesting that the virus entered the brain at a particular time point with concomitant spread through the nervous system (3). In a recent report MV was observed to spread through axonal pathways from initial point infections in the olfactory bulbs in the brains of C57BL/6 mice (53). Progression along olfactory pathways was enhanced in mice which lacked the transporter associated with antigen presentation (TAP) gene. Conversely, in ependymal cells, which lack processes, lateral cell-cell contacts have been suggested as the main means of MV propagation in the CNS of transgenic mice which lack the alpha-beta interferon receptor and express CD46 (34).

Heterotypic coupling between glial cells in the CNS is thought to be common, and this is thought to coordinate the activities of the interconnected cells (59). Astrocytes are known to be closely associated with neuronal synapses and to provide trophic support for synapses (16, 25). Recent studies suggest that astrocytes and neurones communicate reciprocally through nonsynaptic mechanisms (35, 36). Astrocyte-astrocyte contact is so extensive that these cells have been postulated to form a generalized functional syncytium which extends for large distances within the CNS (13). Gap junctions couple astrocytes, and although it would be difficult to imagine MV crossing the junction, the fusogenic nature of the virus may permit cell-to-cell infection at these junctions without a requirement for virus budding. Therefore, we tried to mimic the process-to-process contacts of astrocytes within the brain by utilizing subconfluent GCCM cells for the cell-to-cell spread experiments. EGFP autofluorescence indicates that MV replication and gene expression is occurring within a cell or group of fused cells. Using EGFP, it was possible to make noninvasive observations of MV cell-to-cell spread in real time. In these in vitro experiments, processes were seen to connect the cells, and these mediated the spread of the virus from cell to cell (Fig. 3 and 4). Even though this study was carried out with a single homogeneous monolayer of cells, three different types of infection courses were observed (Fig. 3). The presence of the process-to-process connections appears to produce a connected group of fused cells rather than a typical MV syncytium. In some of these experiments we observed infected cells which were EGFP positive but which did not infect neighboring cells (Fig. 3C). The reason for this is unclear. These cells were clearly surrounded by others which seemed both to be in close contact and to have connecting processes which would be expected to facilitate cell infection. The heterogeneous response in what would be considered to be a homogeneous cell monolayer was an unexpected new observation.

The approaches used in this study will be very useful for observing virus spread between neurones in vivo and may allow the mechanism to be elucidated. We have used a mouse model of MV-induced encephalitis to examine determinants of neurovirulence in the H gene (15). The infection is predominantly neuronal, and in the future it may be possible to utilize this model to examine cell-to-cell spread in vivo with brain slices from animals infected with a recombinant, neurovirulent virus which also expresses the EGFP protein. Here, the virus could function as a tracer of neuronal connections and may indicate whether the hypothesis that MV spreads along specific anatomical pathways is valid. One of the difficulties of studying cell-to-cell spread by MV is that no cell pathogenic effect is observed prior to the obvious fusion and formation of syncytia. MVeGFP now provides an opportunity to study the early stages of MV infection, allowing infected cells to be quickly identified without the need for fixation.

This study has shed light on MV cell-to-cell spread in this important glial cell type. We have shown that the autofluorescence of the reporter gene EGFP is a more sensitive indicator of cell infection than standard ICC methods. Finally, it is clear that MVeGFP will be an invaluable tool for future in vivo studies of MV pathogenesis because of the high levels of transcription which can be obtained upon infection.

ACKNOWLEDGMENTS

We thank Gudrun Christiansen for helpful discussions and invaluable advice on the establishment of the MV rescue system. Additionally, we thank Roy Creighton for photographic work and Paula Haddock for excellent technical assistance. We acknowledge the help of Uta Gassen in critical reading of the manuscript.

This work was supported by the Wellcome Trust (grant 047245) and the Swiss National Science Foundation (no. 31-43475.95).

REFERENCES

1. **Allen, I. V., S. McQuaid, J. McMahon, J. Kirk, and R. McConnell.** 1996. The significance of measles virus antigen and genome distribution in the CNS in SSPE for mechanisms of viral spread and demyelination. J. Neuropathol. Exp. Neurol. **55:**471–480.
2. **Andersson, A. M., and R. F. Pettersson.** 1998. Targeting of a short peptide derived from the cytoplasmic tail of the G1 membrane glycoprotein of Uukuniemi virus (*Bunyaviridae*) to the Golgi complex. J. Virol. **72:**9585–9596.
3. **Baczko, K., J. Lampe, U. G. Liebert, U. Brinckmann, V. ter Meulen, I. Pardowitz, H. Budka, S. L. Cosby, S. Isserte, and B. K. Rima.** 1993. Clonal expansion of hypermutated measles virus in a SSPE brain. Virology **197:**188–195.
4. **Barrett, T., S. M. Subbarao, G. J. Belsham, and B. W. J. Mahy.** 1991. The molecular biology of the morbilliviruses, p. 83–102. *In* D. W. Kingsbury (ed.), The paramyxoviruses. Plenum, New York, N.Y.
5. **Bollo, E., A. Zurbriggen, M. Vandevelde, and R. Fankhauser.** 1986. Canine distemper virus clearance in chronic inflammatory demyelination. Acta Neuropathol. **72:**69–73.
6. **Budka, H., H. Lassmann, and T. Popow-Kraupp.** 1982. Measles virus antigen in panencephalitis. An immunomorphological study stressing dendritic involvement in SSPE. Acta Neuropathol. **56:**52–62.
7. **Bukreyev, A., E. Camargo, and P. L. Collins.** 1996. Recovery of infectious respiratory syncytial virus expressing an additional, foreign gene. J. Virol. **70:**6634–6641.
8. **Cathomen, T., B. Mrkic, D. Spehner, R. Drillien, R. Naef, J. Pavlovic, A. Aguzzi, M. A. Billeter, and R. Cattaneo.** 1998. A matrix-less measles virus is infectious and elicits extensive cell fusion: consequences for propagation in the brain. EMBO J. **17:**3899–3908.
9. **Cathomen, T., H. Y. Naim, and R. Cattaneo.** 1998. Measles viruses with altered envelope protein cytoplasmic tails gain cell fusion competence. J. Virol. **72:**1224–1234.
10. **Cattaneo, R., G. Rebmann, K. Baczko, V. ter Meulen, and M. A. Billeter.**

1987. Altered ratios of measles virus transcripts in diseased human brains. Virology **160:**523–526.
11. **Collins, P. L., M. G. Hill, E. Camargo, H. Grosfeld, R. M. Chanock, and B. R. Murphy.** 1995. Production of infectious human respiratory syncytial virus from cloned cDNA confirms an essential role for the transcription elongation factor from the 5′ proximal open reading frame of the M2 mRNA in gene expression and provides a capability for vaccine development. Proc. Natl. Acad. Sci. USA **92:**11563–11567.
12. **Daoust, P. Y., D. M. Haines, J. Thorsen, P. J. Duignan, and J. R. Geraci.** 1993. Phocine distemper in a harp seal (Phoca groenlandica) from the Gulf of St. Lawrence, Canada. J. Wildl. Dis. **29:**114–117.
13. **Distler, C., Z. Dreher, and J. Stone.** 1991. Contact spacing among astrocytes in the central nervous system: an hypothesis of their structural role. Glia **4:**484–494.
14. **Dubois-Dalcq, M., J. M. Coblentz, and A. B. Pleet.** 1974. Subacute sclerosing panencephalitis. Unusual nuclear inclusions and lengthy clinical course. Arch. Neurol. **31:**355–363.
15. **Duprex, W. P., I. Duffy, S. McQuaid, L. Hamill, S. L. Cosby, M. A. Billeter, J. Schneider-Schaulies, V. ter Meulen, and B. K. Rima.** 1999. The H gene of rodent brain-adapted measles virus confers neurovirulence to the Edmonston vaccine strain. J. Virol. **73:**6916–6922.
16. **Eddleston, M., and L. Mucke.** 1993. Molecular profile of reactive astrocytes—implications for their role in neurologic disease. Neuroscience **54:**15–36.
17. **Escoffier, C., S. Manie, S. Vincent, C. P. Muller, M. A. Billeter, and D. Gerlier.** 1999. Nonstructural C protein is required for efficient measles virus replication in human peripheral blood cells. J. Virol. **73:**1695–1698.
18. **Esiri, M. M., D. R. Oppenheimer, B. Brownell, and M. Haire.** 1982. Distribution of measles antigen and immunoglobulin-containing cells in the CNS in subacute sclerosing panencephalitis (SSPE) and atypical measles encephalitis. J. Neurol. Sci. **53:**29–43.
19. **Fischer, F., C. F. Stegen, C. A. Koetzner, and P. S. Masters.** 1998. Construction of a mouse hepatitis virus recombinant expressing a foreign gene. Adv. Exp. Med. Biol. **440:**291–295.
20. **Foster, T. P., G. V. Rybachuk, and K. G. Kousoulas.** 1998. Expression of the enhanced green fluorescent protein by herpes simplex virus type 1 (HSV-1) as an in vitro or in vivo marker for virus entry and replication. J. Virol. Methods **75:**151–160.
21. **Galinski, M. S., and S. L. Wechsler.** 1991. The molecular biology of the *Paramyxovirus* genus, p. 41–82. *In* D. W. Kingsbury (ed.), The paramyxoviruses. Plenum, New York, N.Y.
22. **Garcin, D., T. Pelet, P. Calain, L. Roux, J. Curran, and D. Kolakofsky.** 1995. A highly recombinogenic system for the recovery of infectious Sendai paramyxovirus from cDNA: generation of a novel copy-back nondefective interfering virus. EMBO J. **14:**6087–6094.
23. **Haas, J., E. C. Park, and B. Seed.** 1996. Codon usage limitation in the expression of HIV-1 envelope glycoprotein. Curr. Biol. **6:**315–324.
23a. **Hangartner, L.** Unpublished data.
24. **Jabbour, J. T., D. A. Duenas, J. L. Sever, H. M. Krebs, and L. Horta-Barbosa.** 1972. Epidemiology of subacute sclerosing panencephalitis (SSPE). A report of the SSPE registry. JAMA **220:**959–962.
25. **Jensen, A., and S.-Y. Chiu.** 1993. Astrocyte networks, p. 309–330. *In* S. Murphy (ed.), Astrocytes: pharmacology and function. Academic Press, San Diego, Calif.
26. **Johnson, G. C., W. R. Fenner, and S. Krakowka.** 1988. Production of immunoglobulin G and increased antiviral antibody in cerebrospinal fluid of dogs with delayed-onset canine distemper viral encephalitis. J. Neuroimmunol. **17:**237–251.
27. **Jons, A., and T. C. Mettenleiter.** 1997. Green fluorescent protein expressed by recombinant pseudorabies virus as an *in vivo* marker for viral replication. J. Virol. Methods **66:**283–292.
28. **Kaelin, K.** 1995. Ph.D. thesis. University of Zurich, Zurich, Switzerland.
29. **Kumanishi, T., and I. Seiichi.** 1979. SSPE: immunohistochemical demonstration of measles virus antigen(s) in paraffin sections. Acta Neuropathol. **48:**161–163.
30. **Liebert, U. G., K. Baczko, H. Budka, and V. ter Meulen.** 1986. Restricted expression of measles virus proteins in brains from cases of subacute sclerosing panencephalitis. J. Gen. Virol. **67:**2435–2444.
31. **Mahalingam, R., M. Wellish, T. White, K. Soike, R. Cohrs, B. K. Kleinschmidt-DeMasters, and D. H. Gilden.** 1998. Infectious simian varicella virus expressing the green fluorescent protein. J. Neurovirol. **4:**438–440.
32. **McQuaid, S., J. Kirk, A. L. Zhou, and I. V. Allen.** 1993. Measles virus infection of cells in perivascular infiltrates in the brain in subacute sclerosing panencephalitis: confirmation by non-radioactive in situ hybridisation, immunocytochemistry and electron microscopy. Acta Neuropathol. **85:**154–158.
33. **Mesquita, R., E. Castanos-Velez, P. Biberfeld, R. M. Troian, and M. M. de Siqueira.** 1998. Measles virus antigen in macrophage/microglial cells and astrocytes of subacute sclerosing panencephalitis. APMIS **106:**553–561.
34. **Mrkic, B., J. Pavlovic, T. Rulicke, P. Volpe, C. J. Buchholz, D. Hourcade, J. P. Atkinson, A. Aguzzi, and R. Cattaneo.** 1998. Measles virus spread and pathogenesis in genetically modified mice. J. Virol. **72:**7420–7427.
35. **Murphy, T. H., L. A. Blatter, W. G. Wier, and J. M. Baraban.** 1993. Rapid communication between neurones and astrocytes in primary cortical cultures. Neuroscience **13:**2672–2679.
36. **Nedergaard, M.** 1994. Direct signalling from astrocytes to neurones in cultures of mammalian brain cells. Science **263:**1768–1771.
37. **Paula-Barbosa, M. M., and C. Cruz.** 1981. Nerve cell fusion in a case of subacute sclerosing panencephalitis. Ann. Neurol. **9:**400–403.
38. **Pearce-Kelling, S., W. J. Mitchell, B. A. Summers, and M. J. Appel.** 1991. Virulent and attenuated canine distemper virus infects multiple dog brain cell types *in vitro*. Glia **4:**408–416.
39. **Pringle, C. R., and A. J. Easton.** 1997. Monopartite negative strand RNA genomes. Semin. Virol. **8:**49–57.
40. **Radecke, F., P. Spielhofer, H. Schneider, K. Kaelin, M. Huber, C. Dotsch, G. Christiansen, and M. A. Billeter.** 1995. Rescue of measles virus from cloned DNA. EMBO J. **14:**5773–5784.
41. **Radecke, F., and M. A. Billeter.** 1996. The nonstructural C protein is not essential for multiplication of Edmonston B strain measles virus in cultured cells. Virology **217:**418–421.
42. **Reed, L. J., and H. Muench.** 1938. A simple method for estimating fifty percent endpoints. Am. J. Hyg. **27:**493–497.
43. **Schneider, H., K. Kaelin, and M. A. Billeter.** 1998. Recombinant measles viruses defective for RNA editing and V protein synthesis are viable in cultured cells. Virology **227:**314–322.
44. **Schneider-Schaulies, S., J. Schneider-Schaulies, M. Bayer, S. Loffler, and V. ter Meulen.** 1993. Spontaneous and differentiation-dependent regulation of measles virus gene expression in human glial cells. J. Virol. **67:**3375–3383.
45. **Schneider-Schaulies, S., U. G. Liebert, K. Baczko, and V. ter Meulen.** 1990. Restricted expression of measles virus in primary rat astroglial cells. Virology **177:**802–806.
46. **Schneider-Schaulies, S., U. G. Liebert, K. Baczko, R. Cattaneo, M. A. Billeter, and V. ter Meulen.** 1989. Restriction of measles virus gene expression in acute and subacute encephalitis of Lewis rats. Virology **171:**525–534.
47. **Schnell, M. J., L. Buonocore, M. A. Whitt, and J. K. Rose.** 1996. The minimal conserved transcription stop-start signal promotes stable expression of a foreign gene in vesicular stomatitis virus. J. Virol. **70:**2318–2323.
48. **Schnell, M. J., T. Mebatsion, and K. K. Conzelmann.** 1994. Infectious rabies viruses from cloned cDNA. EMBO J. **13:**4195–4203.
49. **Spielhofer, P., T. Bachi, T. Fehr, G. Christiansen, R. Cattaneo, K. Kaelin, M. A. Billeter, and H. Y. Naim.** 1998. Chimeric measles viruses with a foreign envelope. J. Virol. **72:**2150–2159.
50. **Singh, M., and M. A. Billeter.** 1999. A recombinant measles virus expressing biologically active human interleukin-12. J. Gen. Virol. **80:**101–106.
51. **Stauber, R. H., and G. N. Pavlakis.** 1998. Intracellular trafficking and interactions of the HIV-1 tat protein. Virology **252:**26–36.
52. **Tober, C., M. Seufert, H. Schneider, M. A. Billeter, I. C. Johnston, S. Niewiesk, V. ter Meulen, and S. Schneider-Schaulies.** 1998. Expression of measles virus V protein is associated with pathogenicity and control of viral RNA synthesis. J. Virol. **72:**8124–8132.
53. **Urbanska, E. M., B. J. Chambers, H. G. Ljunggren, E. Norrby, and H. Kristensson.** 1997. Spread of measles virus through axonal pathways into limbic structures in the brain of TAP1 −/− mice. J. Med. Virol. **52:**362–369.
54. **Valsamakis, A., H. Schneider, P. G. Auwaerter, H. Kaneshima, M. A. Billeter, and D. E. Griffin.** 1998. Recombinant measles viruses with mutations in the C, V, or F gene have altered growth phenotypes in vivo. J. Virol. **72:**7754–7761.
55. **Vandevelde, M., A. Zurbriggen, A. Steck, and P. Bichsel.** 1986. Studies on the intrathecal humoral immune response in canine distemper encephalitis. J. Neuroimmunol. **11:**41–51.
56. **Wertz, G. W., V. P. Perepelitsa, and L. A. Ball.** 1998. Gene rearrangement attenuates expression and lethality of a nonsegmented negative strand RNA virus. Proc. Natl. Acad. Sci. USA **95:**3501–3506.
57. **Whelan, S. P., L. A. Ball, J. N. Barr, and G. T. Wertz.** 1995. Efficient recovery of infectious vesicular stomatitis virus entirely from cDNA clones. Proc. Natl. Acad. Sci. USA **92:**8388–8392.
58. **Yang, T. T., L. Cheng, and S. R. Kain.** 1996. Optimised codon usage and chromophore mutations provide enhanced sensitivity with the green fluorescent protein. Nucleic Acids Res. **15:**4592–4593.
59. **Zahs, K. R.** 1998. Heterotypic coupling between glial cells of the mammalian central nervous system. Glia **24:**85–96.